# Microstrip Leaky-Wave Antenna Using Two Non-Identical Stubs for Enhanced Scan Angle with Enhanced and Consistent Gain

Birendra Kumar, Jayanta Ghosh

*Abstract* – **This paper presents a microstrip leaky-wave antenna using two non-identical stubs per unit length to attain wide-angle frequency beam scanning with enhanced and consistent gain in the operating frequency range. Further, the antenna provides symmetrical scanning, that is, equal scanning angles in both forward and backward directions. The unit cell consists of two open-ended stubs placed at the same side of a microstrip line. Proper impedance matching at broadside frequency is achieved by using two stubs suppressing the open-stopband (OSB) problem. The proposed antenna is an array of 19 unit cells. The array operates in the frequency range 8.6 GHz to 14 GHz with scanning angle 105$^o$ (from -52$^o$ through broadside to +53$^o$) providing a gain of 12.5 dBi to 15.8 dBi in the whole operating band. The radiation efficiency of this antenna is above 64% in the operating frequency range. A prototype is fabricated and measured to experimentally confirm the simulated radiation performances of the proposed antenna.**

*Keywords* – **Microstrip leaky wave antenna, Open stop-band (OSB), Non-identical stubs, Symmetrical scanning.**

## I. INTRODUCTION

A leaky-wave antenna (LWA) is a traveling wave antenna, which can perform narrow beam scanning with frequency without any complicated and costly feed network as typically used in a phased array antenna. Radiation occurs in leaky-wave antenna due to leaking of power into space from the leaky mode in a traveling wave structure supporting fast wave [1]. Because of the scanning feature, LWAs find potential applications in radar imaging, spectrogram analysis, and communications [2].

Periodically modulated guiding structure supporting leaky wave, can radiate in both backward and forward quadrant but, with a common problem of inefficient radiation in the broadside direction. The non-radiation at a narrow region around the broadside direction is known as the open stopband (OSB) problem [3]. The guiding structure can be either a hollow waveguide or a planar microstrip structure with periodic perturbation to realize an LWA. Microstrip structure has several advantages like low profile, low cost, ease of fabrication, and ease of integration, etc. Microstrip LWAs with suppressed OSB using impedance matching is described in [3]-[9]. The reflection-cancellation technique was investigated for OSB suppression in periodic LWAs [4], [9].

*Article history: Received June 15, 2021; Accepted December 14, 2021*

Birendra Kumar and Jayanta Ghosh are at Department of Electronics and Communication Engineering, National Institute of Technology Patna, Patna, Bihar, India, E-mails: birendra.ece17@nitp.ac.in, jghosh@nitp.ac.in

The phase-shifting property of unit cell [10], a complicated multi-layered structure [11], and composite right/left-handed (CRLH) unit cell [12] are studied for seamless scanning. However, CRLH types of LWAs suffer from a problem dispersiveness on cut-off. Recently, microstrip spoof surface plasmon polariton transmission lines have been researched to realize wide-angle scanning LWAs [13]. These LWAs suffer from the problem of limited beam scanning range, asymmetric scanning angle in the forward and backward direction, and inconsistent gain in the operating band.

In [5], a matching stub was employed to suppress the OSB in a microstrip periodic leaky-wave antenna though it suffers from a limited scanning angle problem. The OSB can be mitigated partially using two identical open-ended stubs separated by a quarter-wavelength distance. Later, it was found that the OSB can be completely suppressed with two non-identical elements spaced by about a quarter wavelength [7]. The antennas described in [4]-[7], OSB have been mitigated using open-ended subs but failed to provide seamless, symmetrical, and wide-angle scanning with enhanced and consistent gain in the operating band. In this paper, a microstrip leaky-wave antenna using two non-identical stubs per unit length to attain wide-angle frequency beam scanning with an enhanced and consistent gain is presented. The novelty of this design lies in symmetrical scanning with optimum design of stubs to result in wide impedance bandwidth resulting in wide-angle scanning and introducing more number of stubs per unit cell length to provide higher and consistent gain.

## II. DESIGN OF UNIT CELL

Unit cell design starts with a 50 Ω microstrip line attached with a single open-circuited stub printed on the same dielectric substrate as shown in Fig. 1(a). Dielectric substrate, RO4350, with relative permittivity ($\varepsilon_r$) 3.66, thickness 0.762 mm, and loss tangent (tanδ), 0.004 is used. The attenuation constant ($\alpha_{eff}$) and phase constant ($\beta_{eff}$) of the unit cell can be obtained from the scattering parameter information with the use of the following equations [9]

$$\alpha_{eff} = \frac{1}{p}\mathrm{Im}\left[\cos^{-1}\left(\frac{1-S_{11}S_{22}+S_{21}S_{12}}{2S_{21}}\right)\right], \quad (1)$$

$$\beta_{eff} = \frac{1}{p}\mathrm{Re}\left[\cos^{-1}\left(\frac{1-S_{11}S_{22}+S_{21}S_{12}}{2S_{21}}\right)\right]. \quad (2)$$

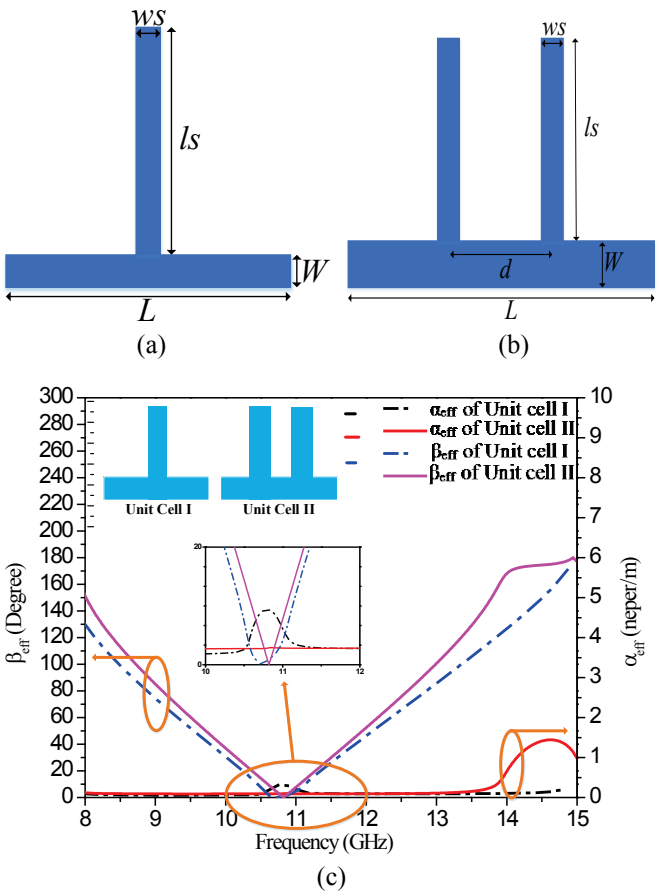


Fig. 1. (a) Top view of unit cell-I, (b) Top view of unit cell-II with $L$ = 16 mm, $W$ = 1.67 mm, $ls$ = 7.5 mm, $ws$ = 1 mm, $d$ = 3.5 mm, (c) Dispersion diagram corresponds to unit cell described in (a)&(b).

The unit cell containing a microstrip line with an open stub is simulated using electromagnetic simulator HFSS. Fig. 1(c) reveals that unit cell containing single stub produces high attenuation at frequency 10.8 GHz resulting open stop band problem. The high attenuation is due to the electromagnetic waves reflected by the stub towards the input source. Reflection arising from a single stub can be balanced by introducing another stub placed at a quarter wavelength apart from the first stub (Fig. 1(b)). The phase difference between the reflected waves generated due to the stubs depends on the different path lengths traveled by the reflections. The phase difference between reflections, $\Delta\phi$ is given by [4],

$$\Delta\phi = \beta_n (2d) = \pi \text{ , where } d = \lambda / 4 \text{ .} \quad (3)$$

Reflection from the second stub travels half wavelength (quarter wavelength for incident wave and quarter wavelength for reflected waves) more distance than the reflection from the first stub. Due to this half-wavelength path difference, the phase difference between the two reflected waves calculated by Eq. (3) is 180°. This means that the reflected waves coming out from each stub are in out of phase resulting in minimum power reflections towards the source. These reflected waves get canceled if the amplitudes of the reflected wave coming from the two stubs become the same. Reflection cancellation keeps αeff relatively small. A plot of frequency versus attenuation constant for this double stub unit cell is shown in Fig. 1(c). The figure clearly shows the reduction in attenuation constant at the center frequency. Hence OSB is suppressed by canceling the reflections. In Fig. 1(c), the plot of effective phase constant ($\beta_{eff}$), shows that throughout the operating band phase constant varies linearly fulfilling the requirement of the leaky-wave antenna in the case of the double stubbed unit cell.

## III. Equivalent Circuit Analysis

The equivalent electrical circuit of the proposed unit cell is investigated to get further insight. The equivalent circuit for the proposed unit cell can be formulated with the use of the planar waveguide model given in [1], [18]. For the circuit formulation, the unit cell is considered as cascading of five sections as shown in Fig. 2(a). Section a, c, e is the transmission line of impedance 50 Ω whereas section b, d is the T-junction. The complete equivalent circuit of the double stubbed unit cell is shown in Fig. 2(b). The equivalent circuit of a T-junction has shunt impedance $jB_T$. The shunt impedance $B_T$ may be determined by using the following equation [1], [18]

$$B_T = \frac{Y_{02}}{\lambda_1} D_1 5.5 \frac{\varepsilon_r + 2}{n^2 \varepsilon_r} \left[ 1 + 0.9 \ln \frac{Z_{01}}{Z_{02}} + 4.5 \frac{Z_{01}}{Z_{02}} \left( \frac{f}{f_{p1}} \right)^2 - 4.4 e^{\left( -1.3 \frac{Z_{01}}{Z_{02}} \right)} - 20 \left( \frac{Z_{02}}{n_0} \right)^2 \right] \frac{d_1}{D_2}, \quad (4)$$

where $Z_{01}$ is main arm characteristic impedance, $Z_{02}$ is sidearm characteristic impedance, $Y_{02}$ is sidearm characteristic admittance, $D_i$ equivalent parallel plate line width where $i$ represent series and shunt lines. $\varepsilon_r$ is the permittivity of the material, $f_p$ first higher-order mode cut-off frequency, $\lambda_i$ guided wavelength of the microstrip line, n is the coupling factor. The shunt impedance $B_T$ at center frequency is calculated as $B_T = -5.20 \cdot 10^{-4}\ \Omega$. Using this value of $B_T$ input impedance seen at the input terminal of the circuit can be calculated. The impedance at the input terminal of the unit cell using the impedance of different sections of the microstrip line and T-junction is estimated as approximately 50 Ω at the center frequency. Thus, impedance matching is achieved at broadside frequency minimizing the electro-magnetic reflections going back to the source. This explains the suppression of OSB using two open-ended stubs.

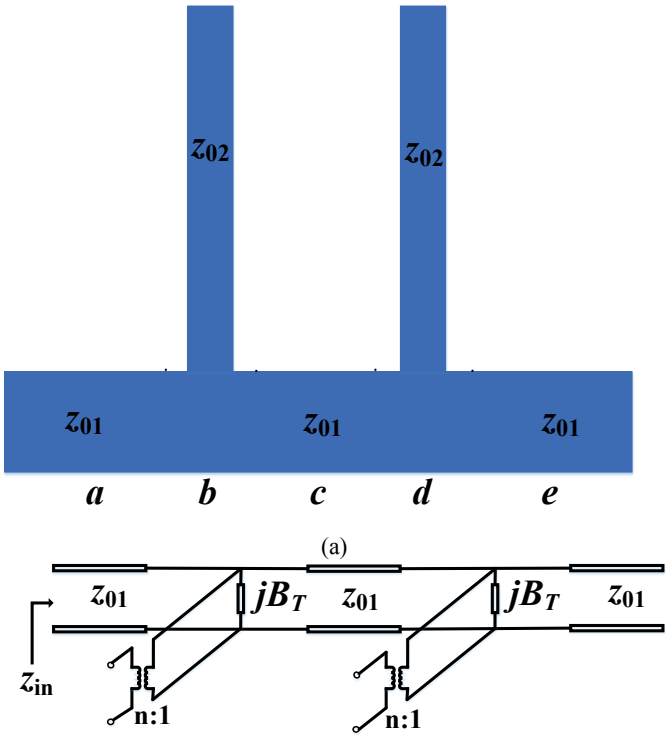


Fig. 2. Unit cell with dual stub: (a) Planar structure, (b) Equivalent circuit.

## IV. FULL-LENGTH STRUCTURE

After finalizing the design of the unit cell, an array of length $9\lambda_g$ is designed, where $\lambda_g$ is the guided wavelength corresponding to the lowest operating frequency. Gain of the array can be increased by introducing more number stubs keeping the array length fixed. First, a 10-unit cell at the same side of the microstrip as shown in Fig. 3(a) is designed.

As the frequency increases the gain starts decreasing as it is shown in Fig. 4. To increase the gain and make it consistent, the radiator is increased keeping the length same. More stubs can be fixed by reducing the periodicity. Periodicity can be made half by placing the stubs of adjacent unit cells oppositely [8]. The array having 19-unit cells in which ten are on the same side of the microstrip and nine are on the opposite side of the microstrip is designed as shown in Fig. 3(b). Here periodicity becomes half of the periodicity utilized for unit cell design in section 2. The equal stub length array suffers from the problem of impedance mismatch at broadside direction as shown in Fig. 4 and Fig. 5(b). Stub lengths are optimized to get impedance matching at broadside frequency resulting in unequal stub lengths. Thus, an array of 19-unit cells with two non-identical stubs (unequal stub length) of array length $9\lambda g$ is designed shown in Fig. 5(a), to provide enhanced and consistent gain in the operating frequency band.

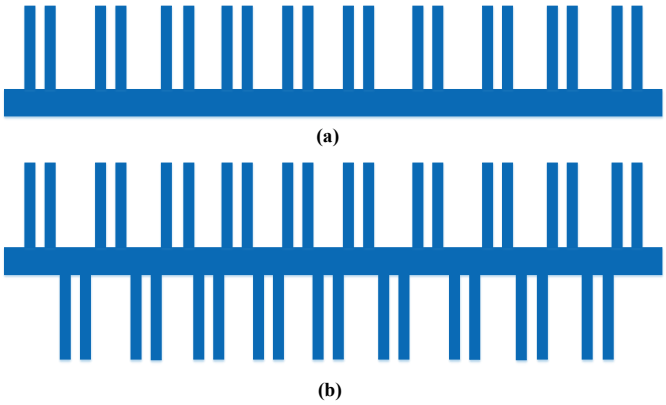


Fig. 3. (a) Array of equal stub 10-unit cell, (b) Array of equal stub 19-unit cell.

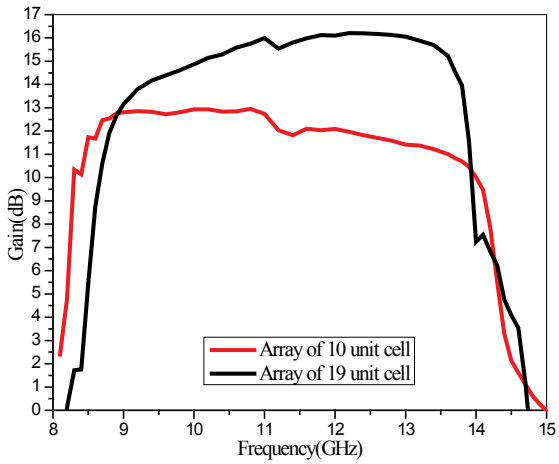


Fig. 4. Gain plot of the array of 10-unit cell and 19-unit cell.

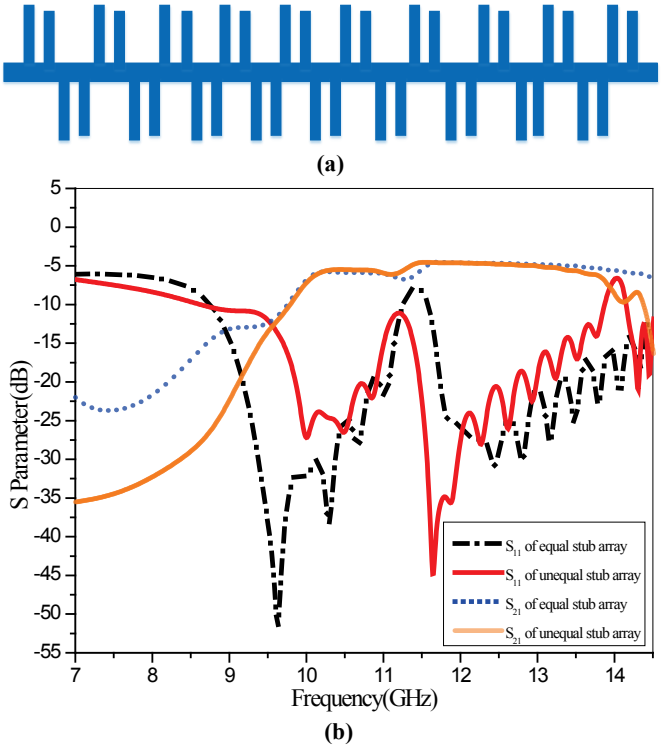


Fig. 5. (a) Array of unequal stub 19-unit cell, (b) Simulated S parameter of equal stub and unequal stub array.

## V. Results and Discussions

Finally, a prototype (Fig. 6) of the proposed antenna is fabricated and measurements are done.

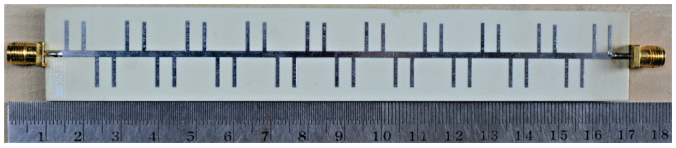

Fig. 6. Fabricated prototype view.

The simulated S parameters are in good agreement with that of measured as shown in Fig. 7(a). The slight variation between the simulated and measured results may be because of fabrication and measurement imperfections. Fig. 7(b) shows the radiation pattern at five different frequencies. The antenna can scan from -52° to +53° [105° scanning angle] operating from 8.6 GHz to 14 GHz as shown in Fig. 8. The radiation efficiency is above 64% in the operating range as shown in Fig. 9. The antenna can scan equally the left and right sides of the broadside direction resulting in symmetrical scanning. The measured gain in the operating frequency varies from 12.5 dBi to 15.8 dBi providing 3.3 dBi gain variation shown in Fig. 8.

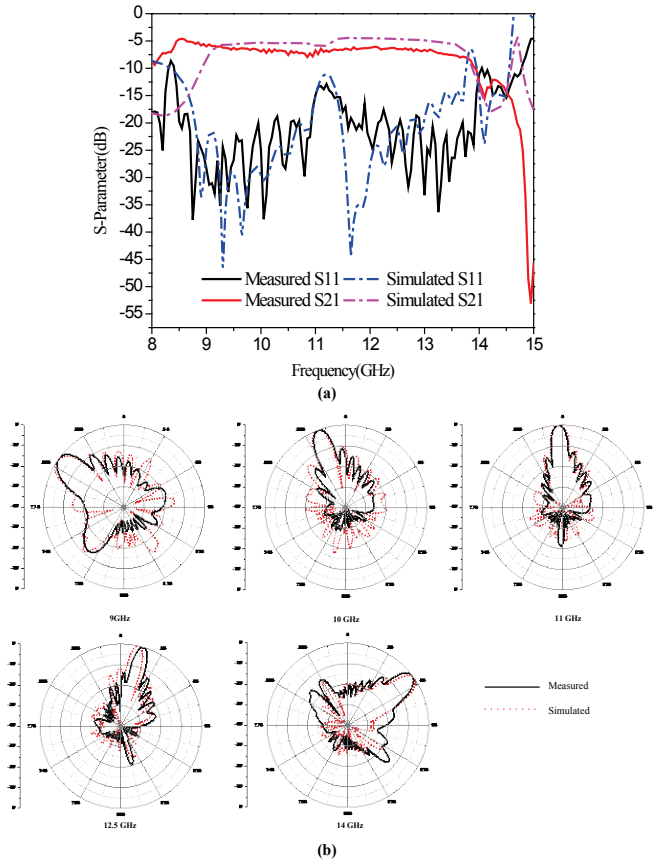


Fig. 7. Measured and simulated: (a) S-parameters and (b) radiation patterns at frequency 9 GHz, 10 GHz, 11 GHz, 12.5 GHz, 14 GHz.

The proposed antenna has been compared with some similar kind of work available in the literature in Table I. The table shows proposed antenna gives wider beam scanning with almost consistent gain with the smallest array length. $\lambda$g Corresponds to the lowest operating frequency. This antenna provides enhanced gain. Some of the antennae provide more gain, but those are having much higher array lengths.

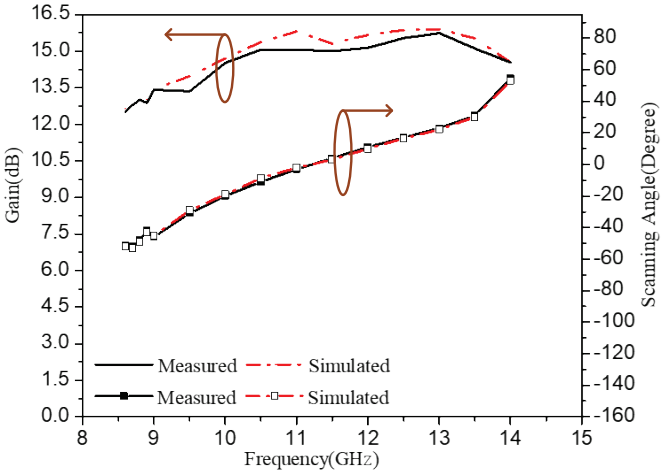


Fig. 8. Measured & simulated gain and scanning angle of the proposed antenna.

TABLE I
COMPARISON OF PROPOSED WORK WITH STATE OF ART OTHER REPORTED WORKS

| Ref. | Frequency Range (GHz) | Antenna Length | Scanning Range (Scan Angle) | Gain range (dBi) (Gain variation) |
|---|---|---|---|---|
| [6] | 9.7-10.3 | 16 $\lambda_g$ | $-2^0$ to $0.3^0$ ($2.3^0$) | 20-21 (1) |
| [5] | 25-26 | 10 $\lambda_g$ | $-5^0$ to $5^0$ ($10^0$) | 14-15 (1) |
| [15] | 50-85 | 10 $\lambda_g$ | $-9^0$ to $40^0$ ($49^0$) | 9.1-14.2 (5.1) |
| [9] | 8.5-14 | 11 $\lambda_g$ | $-32^0$ to $20^0$ ($52^0$) | 13.97-15.4 (1.43) |
| [11] | 8.9-10.6 | 16 $\lambda_g$ | $-27.5^0$ to $46^0$ ($73.5^0$) | 13-15.5 (2.5) |
| [13] | 5-7 | 15 $\lambda_g$ | $-30^0$ to $51^0$ ($81^0$) | 15.9-19.4 (3.5) |
| [16] | 13-19.45 | 10 $\lambda_g$ | $-48^0$ to $35^0$ ($83^0$) | 10-13 (3) |
| [14] | 22-28 | 15 $\lambda_g$ | $-44^0$ to $40^0$ ($84^0$) | 8-12 (4) |
| [10] | 8.3-10.9 | 18 $\lambda_g$ | $-60^0$ to $30^0$ ($90^0$) | 13-16.87 (3.87) |
| [17] | 20-29 | 15 $\lambda_g$ | $-50^0$ to $45^0$ ($95^0$) | 9.2-12.2 (3) |
| **This work** | **8.6-14** | **9$\lambda_g$** | **$-52^0$ to $53^0$ ($105^0$)** | **12.5-15.8 (3.3)** |

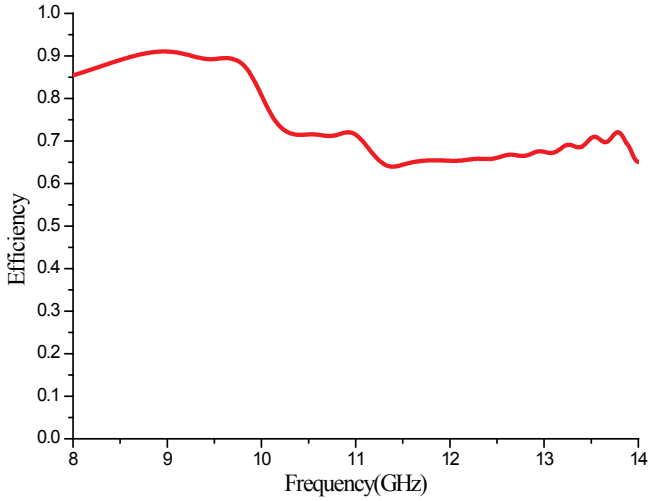


Fig. 9. Radiation efficiency of the proposed antenna.

## VI. CONCLUSION

The unit cell of the proposed antenna is made of dual stubs attached with a microstrip line. An antenna array of 19 such unit cells is designed. The compact design of the antenna is achieved which provides a scanning angle of 105° symmetrically in the backward and forward direction. The antenna provides a consistent gain in the operating band 8.6 GHz to 14 GHz with a peak gain of 15.8 dBi. The antenna can be very much useful for applications where beam scanning is in demand.

## REFERENCES

[1] A. A. Oliner and D. R. Jackson, "Leaky-Wave Antennas" in *Antenna Engineering Handbook*, 4th ed., New York, NY, USA, Mc-Graw-Hill, 2007.

[2] G. Zhang, Q. Zhang, S. Ge, Y. Chen, and R. D. Murch, "High Scanning-Rate Leaky-Wave Antenna Using Complementary Microstrip-Slot Stubs", *IEEE Transactions on Antennas and Propagation*, vol. 67, no. 5, pp. 2913-2922, May 2019.

[3] R. Ranjan and J. Ghosh, "SIW-Based Leaky-Wave Antenna Supporting Wide Range of Beam Scanning Through Broadside", *IEEE Antennas and Wireless Propagation Letters*, vol. 18, no. 4, pp. 606-610, April 2019.

[4] M. Guglielmi and D. R. Jackson, "Broadside Radiation from Periodic Leaky-Wave Antennas", *IEEE Transactions on Antennas and Propagation*, vol. 41, no. 1, pp. 31-37, Jan. 1993.

[5] S. Paulotto, P. Baccarelli, F. Frezza, and D. R. Jackson, "A Novel Technique for Open-Stopband Suppression in 1-D Periodic Printed Leaky-Wave Antennas", *IEEE Transactions on Antennas and Propagation*, vol. 57, no. 7, pp. 1894-1906, July 2009.

[6] J. T. Williams, P. Baccarelli, S. Paulotto, and D. R. Jackson, "1-D Leaky-Wave Antenna with the Open-Stopband Suppressed: Design Considerations and Comparisons with Measurements", *IEEE Transactions on Antennas and Propagation*, vol. 61, no. 9, pp. 4484-4492, Sept. 2013.

[7] J. Liu, W. Zhou, and Y. Long, "A Simple Technique for Open-Stopband Suppression in Periodic Leaky-Wave Antennas Using Two Nonidentical Elements per Unit Cell", *IEEE Transactions on Antennas and Propagation*, vol. 66, no. 6, pp. 2741-2751, June 2018.

[8] Y.-L. Lyu, X.-X. Liu, P.-Y. Wang, D. Erni, Q. Wu, C. Wang, N.-Y. Kim, and F.-Y. Meng, "Leaky-Wave Antennas Based on Noncutoff Substrate Integrated Waveguide Supporting Beam Scanning From Backward to Forward", *IEEE Transactions on Antennas and Propagation*, vol. 64, no. 6, pp. 2155-2164, June 2016.

[9] B. Kumar, R. Ranjan, and J. Ghosh, "Novel Printed Leaky-Wave Antenna with Suppressed OSB for Broad Angle Scanning", 2019 TEQIP III Sponsored *International Conference on Microwave Integrated Circuits, Photonics and Wireless Networks (IMICPW)*, Tiruchirappalli, India, pp. 361-364, 2019.

[10] L. Jidi, X.-Y. Cao, X. Zhu, and B. Zhu, "Printed Frequency Scanning Antenna Array with Wide Scanning Angle Range", *Progress In Electromagnetics Research Letters*, vol. 77, pp. 117-122, 2018.

[11] L. Cui, W. Wu and D. Fang, "Printed Frequency Beam-Scanning Antenna with Flat Gain and Low Sidelobe Levels", *IEEE Antennas and Wireless Propagation Letters*, vol. 12, pp. 292-295, 2013.

[12] P. Pan, F.-Y. Meng, and Q. Wu, "A Composed Right/Left-Handed Waveguide with Open-Ended Corrugations for Backward-to-Forward Leaky-Wave Antenna Application", *Microwave and Optical Technology Letters*, vol. 50, no. 3, pp. 579-582, March 2008.

[13] D. Wei, J. Li, J. Yang, Y. Qi, and G. Yang, "Wide-Scanning-Angle Leaky-Wave Array Antenna Based on Microstrip SSPPs-TL", *IEEE Antennas and Wireless Propagation Letters*, vol. 17, no. 8, pp. 1566-1570, Aug. 2018.

[14] M. H. Rahmani and D. Deslandes, "Circularly Polarised Periodic Leaky-Wave Antenna with Filtering Capability", *IET Microwaves, Antennas & Propagation*, vol. 12, no. 11, pp. 1811-1815, September 2018.

[15] X. Bai, S. W. Qu, K.-B. Ng, and C. H. Chan, "Sinusoidally Modulated Leaky-Wave Antenna for Millimeter-Wave Application", *IEEE Transactions on Antennas and Propagation*, vol. 64, no. 3, pp. 849-855, March 2016.

[16] Y. Lyu, F. Meng, G. Yang, Q. Wu, and K. Wu, "Leaky-Wave Antenna With Alternately Loaded Complementary Radiation Elements," *IEEE Antennas and Wireless Propagation Letters*, vol. 17, no. 4, pp. 679-683, April 2018.

[17] M. H. Rahmani and D. Deslandes, "Backward to Forward Scanning Periodic Leaky-Wave Antenna with Wide Scanning Range", *IEEE Transactions on Antennas and Propagation*, vol. 65, no. 7, pp. 3326-3335, July 2017.

[18] R. Garg, P. Bhartia, I. Bahl, and A. Ittipiboon, *Microstrip Antenna Design Handbook*, MA, Norwood: Artech House, p. 320, 2001.